Drug Development and Industrial Pharmacy, 23(1), 81-93 (1997)

RESEARCH PAPER

New Parameters Derived from Tablet Compression Curves. Part II. Force-Displacement Curve

Osmo K. Antikainen and Jouko K. Yliruusi

Pharmaceutical Technology Division, University of Helsinki, PO Box 56, Viikinkaari 5, FIN-00014 Helsinki, Finland

ABSTRACT

Previously, many authors have described different types of parameters derived from tablet compression force-time curves. In this study, a great number of new compression parameters were calculated from tablet force-displacement curves. Tablets were made with an instrumented eccentric tablet machine using three different compression forces and three compression speeds, and α-lactose monohydrate as a model material. The results showed that the presented new force-displacement parameters explain the compression phenomenon from different points of view. The final usefulness of these parameters together should be studied in the future with different types of materials. It is expected that many of the presented parameters can give valuable information on tablet compression and can lay the foundation for understanding of the compression phenomenon and bond formation during tableting.

INTRODUCTION

Previously, many authors have presented papers on tablet force-time compression curves (1-4). Also, an increasing number of publications concerning the evaluation of the force-displacement curves have been presented (5-8). Typically these publications have analyzed force-displacement compression curves mainly quantitatively, although more recently some advanced analyses have been presented (9-11).

Another field in studying the compression profiles is to parameterize the force-displacement curves. Still today it seems that there are no generally accepted parameters which are superior to the others. This may be the basic nature of the problem. The general usefulness of the parameterization of force-displacement curves may

require the simultaneous use of different—and new—parameters and the application of the most modern modeling techniques.

The primary purpose of this study was to present many new compression parameters calculated from tablet force–displacement curves and to explain the crushing strength and friability of lactose tablets using these parameters.

MATERIALS AND METHODS

The materials and methods have been described in Part I of this series (this issue). The material, α-lactose monohydrate (80 mesh) with 1% of magnesium stearate, was compressed to tablets using an eccentric tablet machine. The width of the flat-faced tablets was 9 mm and the target height was 4.0 mm. Compression forces were 11, 15, and 19 kN; and compression speeds 10, 20, and 40 rpm. Compression parameters were calculated from 5 parallel compression cycles. The responses of tablets were crushing strength and friability.

Table 1

Parameters Calculated from the Force–Displacement Compression Curves

Parameter	Symbol	Unit
Upper punch force	F_{up}	N
Lower punch force	F_{lp}	N
Effective force	F_{eff}	N
Maximum of the effective force	$F_{eff,max}$	N
Maximum upper punch force	$F_{up,max}$	N
Maximum lower punch force	$F_{lp,max}$	N
Maximum punch displacement	S_{max}	mm
Punch displacement when the force is detected (F_{eff} > 50 N)	S_0	mm
Force–displacement ratio	R_{FD}	—

Description of Calculated Compression Parameters

The raw force–displacement data were filtered using floating 5-point smoothing. The summary of the calculated compression parameters is given in Tables 1–4. The calculation of the parameters was made with Mathcad v. 5.0 Plus (Math Soft Inc., USA), regression modeling with MODDE v. 3.0 (Umetri AB, Sweden), and the figures with SigmaPlot v. 2.01 (Jandel Scientific GmbH, Germany).

Theory and Equations for Parameters Calculated from Tablet Force–Displacement Compression Curves

Effective force F_{eff} is calculated as a geometrical average mean [Eq. (1)] of upper punch force F_{up} and lower punch force F_{lp} as presented earlier (Part I of this series). It is assumed here that the use of effective force will minimize the effects of unhomogenous structure of compressed tablets caused by die wall friction, particle rearrangement, and different types of deformation (12).

$$F_{eff} = \sqrt{F_{up}F_{lp}} \quad (1)$$

The symbols for quartiles of the increasing part of the force–displacement curve are given in Table 2 and the idea is described in Figs. 1 and 2. The following three

Table 2

Quartiles of Distances for the Force–Displacement Curves

Parameter	Symbol	Unit
Quartiles for the increasing part (FI) of the force–displacement curve		
25% quartile for the FI curve	S_{FIQ25}	mm
50% quartile for the FI curve	S_{FIQ50}	mm
75% quartile for the FI curve	S_{FIQ75}	mm
Quartiles for the decreasing part (FD) of the force–displacement curve		
25% quartile for the FD curve	S_{FDQ25}	mm
50% quartile for the FD curve	S_{FDQ50}	mm
75% quartile for the FD curve	S_{FDQ75}	mm

Table 3

Ratios of Different Quartiles Calculated from the Force-Displacement Curves

Parameter	Symbol
Ratios of the quartiles of the FI compression curves[a]	
25% quartile ratio of the FI curve	$RFI_{Q25,Feff,max}$
50% quartile ratio of the FI curve	$RFI_{Q50,Feff,max}$
75% quartile ratio of the FI curve	$RFI_{Q75,Feff,max}$
Ratios of the quartiles of the FD compression curves[a]	
25% quartile ratio of the FI curve	$RFD_{Q25,Feff,max}$
50% quartile ratio of the FI curve	$RFD_{Q50,Feff,max}$
75% quartile ratio of the FI curve	$RFD_{Q75,Feff,max}$
Ratios of the FI and FD quartiles of the compression curves	
Ratio for the first quartiles	$R25_{FI,FD}$
Ratio for the second quartiles	$R50_{FI,FD}$
Ratio for the third quartiles	$R75_{FI,FD}$
Normalized ratios of quartiles of the FI compression curves	
25% normalized ratio for the FI curve	$NRFI_{Q25}$
50% normalized ratio for the FI curve	$NRFI_{Q50}$
75% normalized ratio for the FI curve	$NRFI_{Q75}$
Normalized ratios of quartiles of the FD compression curves	
25% normalized ratio for the FD curve	$NRFD_{Q25}$
50% normalized ratio for the FD curve	$NRFD_{Q50}$
75% normalized ratio for the FD curve	$NRFD_{Q75}$

[a]Symbols FI and FD are defined in Table 2.

Table 4

Parameters Calculated from the Effective Work Curve

Parameter	Symbol	Unit
Effective work force	F_{weff}	N
Maximum force for the F_{Weff} curve	$F_{Weff,max}$	N
Effective work	W_{eff}	J
Distance when $F_{Weff,max}$ is achieved	$S_{FWeff,max}$	mm
Distance when 50% quartile of the increasing part in effective work curve is achieved	S_1	mm
Distance when 50% quartile of the decreasing part in effective work curve is achieved	S_2	mm
Normalized S_1	Ns_1	—
Normalized S_2	Ns_2	—
Ratio of $S_2 - S_1$ to $S_{max} - S_0$	S_{REL}	—
Area of the left side in effective work curve in regard to the peak.	A_L	J
Area of the right side in effective work curve in regard to the peak.	A_R	J
Ratio of A_L to hole area under effective work curve	φ_1	—
Ratio of A_R to A_L	φ_2	—
Normalized $F_{Weff,max}$	$Ns_{FWeff,max}$	—
Normalized $F_{Weff,max}$	$NF_{Weff,max}$	—
Ratio for $S_{FWeff,max}$	$Rs_{FWeff,max}$	—

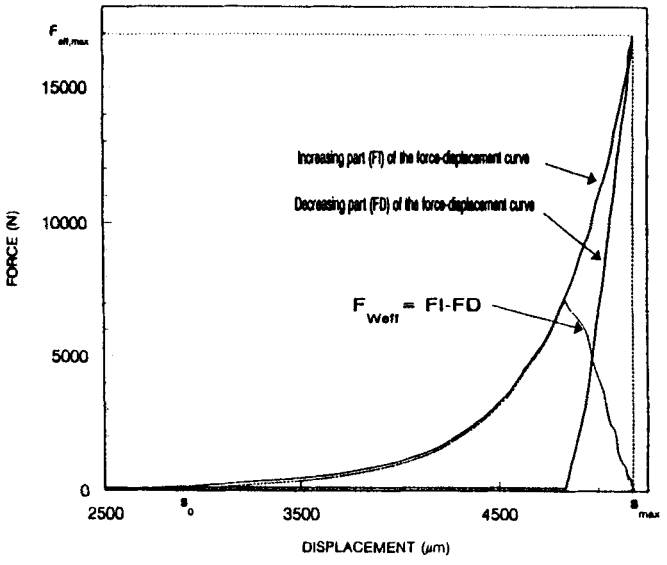

Figure 1. Basic force–displacement curve. Effective compression force (F_{eff}) as a function of upper punch displacement.

equations [Eqs. (2)–(4)] give the corresponding ratios against the difference $S_{max} - S_0$ (See Table 1).

$$RFI_{Q25,Feff,max} = \frac{S_{FIQ25} - S_0}{S_{max} - S_0} \quad (2)$$

$$RFI_{Q50,Feff,max} = \frac{S_{FIQ50} - S_0}{S_{max} - S_0} \quad (3)$$

$$RFI_{Q75,Feff,max} = \frac{S_{FIQ75} - S_0}{S_{max} - S_0} \quad (4)$$

Similar ratios were calculated also for the decreasing part of the force–displacement curves, as follows [Eqs. (5)–(7); Fig. 2):

$$RFD_{Q25,Feff,max} = \frac{S_{FDQ25} - S_0}{S_{max} - S_0} \quad (5)$$

$$RFD_{Q50,Feff,max} = \frac{S_{FDQ50} - S_0}{S_{max} - S_0} \quad (6)$$

$$RFD_{Q75,Feff,max} = \frac{S_{FDQ75} - S_0}{S_{max} - S_0} \quad (7)$$

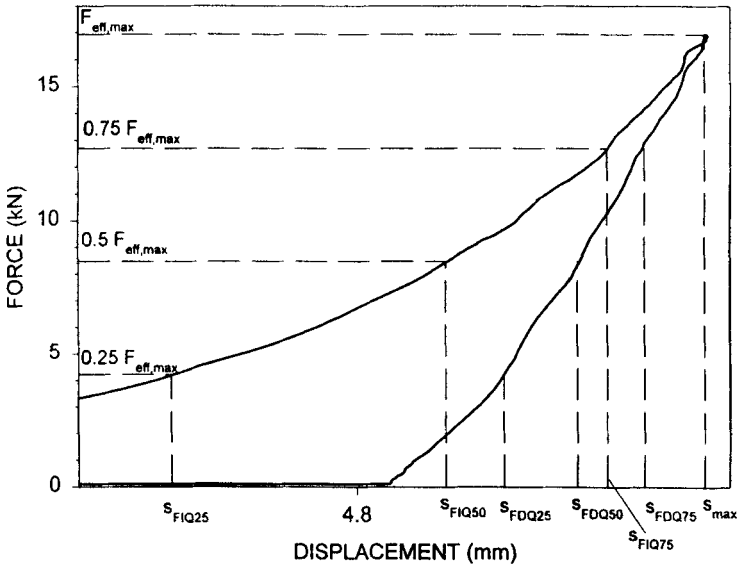

Figure 2. A detailed figure of effective compression force as a function of upper punch displacement.

All calculated parameters presented in Eqs. (2)–(7) were also normalized with the maximum effective force [see Eqs. (8)–(13)] because bond formation during tableting is evidently a complicated nonlinear function of the maximum effective force. Therefore this kind of normalization may give additional information on the compression behavior of materials.

$$NRFD_{Q25} = \frac{RFD_{Q25,Feff,max}}{F_{eff,max}} \quad (8)$$

$$NRFD_{Q50} = \frac{RFD_{Q50,Feff,max}}{F_{eff,max}} \quad (9)$$

$$NRFD_{Q75} = \frac{RFD_{Q75,Feff,max}}{F_{eff,max}} \quad (10)$$

$$NRFI_{Q25} = \frac{RFI_{Q25,Feff,max}}{F_{eff,max}} \quad (11)$$

$$NRFI_{Q50} = \frac{RFI_{Q50,Feff,max}}{F_{eff,max}} \quad (12)$$

$$NRFI_{Q75} = \frac{RFI_{Q75,Feff,max}}{F_{eff,max}} \quad (13)$$

Ratios of the increasing and decreasing parts of the compression curves were calculated according to Eqs. (14)–(16). These ratios were determined because they give information on the elastic behavior of materials. For an ideal rubber-elastic material all these ratios will be 1, but in practice the values are always less than 1.

$$R25_{FI,FD} = \frac{S_{FIQ25}}{S_{FDQ25}} \quad (14)$$

$$R50_{FI,FD} = \frac{S_{FIQ50}}{S_{FDQ50}} \quad (15)$$

$$R75_{FI,FD} = \frac{S_{FIQ75}}{S_{FDQ75}} \quad (16)$$

Also the ratio R_{FD} between the maximum effective force and maximum punch displacement was determined. It is assumed that this parameter may give information on the compactibility of materials. If material forms a week needle-like network (like mannitol), which resists the upper punch displacement less than more spherical particles (like lactose and glucose), this ratio will be able to detect the difference between the materials.

$$R_{FD} = \frac{F_{eff,max}}{S_{max} - S_0} \quad (17)$$

Parameters Calculated from the Effective Work Force Curve

Effective work force is defined as follows:

$$F_{Weff} = F_{eff,FI} - F_{eff,FD} \quad (18)$$

and it describes quite well the force, which is used for the irreversible deformations. In theory it is still possible that the die wall friction may to some extent contribute to the value, because it is evidently different during the compression and ejection phases. The form of this parameter is seen in Fig. 3 (and in Fig. 1). The area under the curve, effective work, is calculated directly using the following integral:

$$W_{eff} = \int_{S_0}^{S_{max}} F_{Weff}\, ds \quad (19)$$

The higher the value, the more work has been found in the formation of the tablet. For a rubber-elastic system—where no bondings are formed—the value is naturally 0.

Also the ratio of the effective work force (Table 4) and the maximum of the effective force (Table 1) was calculated, and it was named normalized $F_{Weff,max}$ [Eq. (20)].

$$NF_{Weff,max} = \frac{F_{Weff,max}}{F_{eff,max}} \quad (20)$$

The value of this parameter is obviously limited to description of the compression behavior of a single material, and the parameter is expected to have only a limited value if different materials are compared.

The ratio $Rs_{FWeff,max}$ is defined in Eq. (21). This parameter is related to the irreversible deformation in

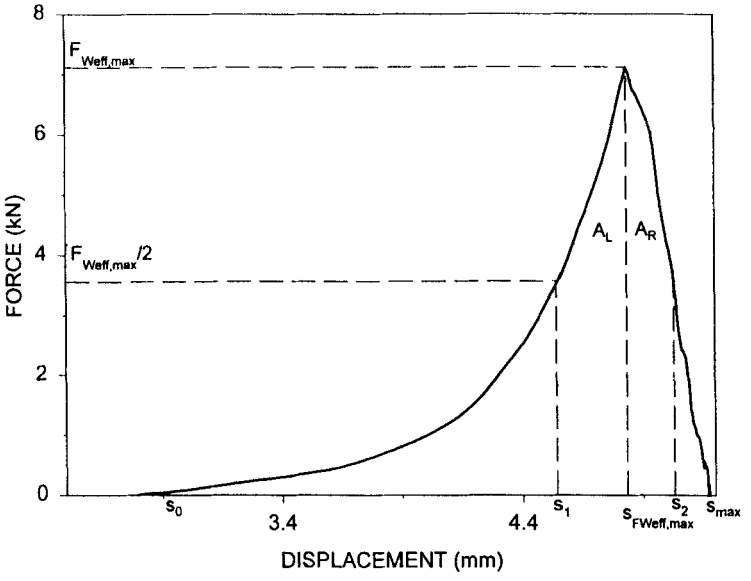

Figure 3. Effective work force as a function of upper punch displacement.

tablet compression. The parameter can classify the materials into plastic and fragmented. For fragmented materials the numerical value will approach 1, but for more plastic systems the value will be smaller.

$$Rs_{\mathrm{FWeff,max}} = \frac{S_{\mathrm{FWeff,max}} - S_0}{S_{\max} - S_0} \tag{21}$$

Normalized 50% quartiles for the increasing [Eq. (22)] and decreasing part [Eq. (23)] of the effective work force curve are defined next. s_1 and s_2 are punch displacements when 50% quartiles of the work force curve are reached (see Fig. 3).

$$Ns_1 = \frac{S_1 - S_0}{S_{\max} - S_0} \tag{22}$$

$$Ns_2 = \frac{S_2 - S_0}{S_{\max} - S_0} \tag{23}$$

The ability of the parameter Ns_1 to explain crushing strength and friability is poor; it can, however, reflect some time-dependent behaviour of the elastic materials and can be used in neural net models.

The parameter Ns_2 approaches 1 for very fragmented materials and, as the material acts more elastically during compression, the term Ns_2 has lower values. The term S_{REL} in Eq. (24) is the ratio of the punch displacement differences as the 50% quartiles of the effective work force curve reach the difference between $S_{\max}$ and S_0.

The term seems to have higher values when more elastic materials are used.

$$S_{\mathrm{REL}} = \frac{S_2 - S_1}{S_{\max} - S_0} \tag{24}$$

In the following are defined the absolute areas A_{L} and A_{R} in the effective work force curve (see Fig. 2):

$$A_{\mathrm{L}} = \int_{S_0}^{S_{\mathrm{FWeff,max}}} F_{\mathrm{Weff}}\, ds \tag{25}$$

$$A_{\mathrm{R}} = \int_{S_{\mathrm{FWeff,max}}}^{S_{\max}} F_{\mathrm{Weff}}\, ds \tag{26}$$

The last terms [Eqs. (27) and (28)] define two different ratios of areas (A_{L} and A_{R}) described above.

$$\varphi_1 = \frac{A_{\mathrm{L}}}{A_{\mathrm{L}} + A_{\mathrm{R}}} \tag{27}$$

where φ_1 approaches a value of 1 in compression when materials are very plastic. For more elastic materials the term will have lower values.

$$\varphi_2 = \frac{A_R}{A_L} \tag{28}$$

Here φ_2 approaches 0 for materials which undergoes very irreversible deformation and with higher values of the term the material will act in a more elastic way. The general applicability of parameters φ_1 and φ_2, like many others given above, will certainly require many additional experiments and accurate evaluation with different types of materials.

RESULTS AND DISCUSSION

An example of the force–displacement curve (effective compression force, F_{eff}, as a function of upper punch displacement) is given in Fig. 1. Also the effective work force curve [Table 4; Eq. (19)] is shown in Fig. 1. The lower limit in the integration was S_0 ($F_{eff} <$ 50 N). The few parameters calculated from the effective work force curve are presented in more detail in Fig. 3.

Figure 2 shows the the quartiles of the increasing part (FI) and the decreasing part (FD) of the force–displacement curve. Also the corresponding upper punch displacements are shown in this figure. It is obvious that the structure of the curve is highly dependent on the compression force and compression speed, and certainly on the material used. Thus these parameters are probably able to characterize simultaneously the behavior of material during compression better than just rough effective work. If in the future, even these parameters prove too rough, it will be possible to use the different ratios of the quartiles of the FI and FD curves (Table 3) or use proper normalization (Table 3). It will be easy also to calculate different partial areas and their ratios from the curves. We have not done it here, mainly because the number of parameters to be tested is already quite large. All the above-mentioned three figures (Figs. 1–3) illustrate the same real compression cycle.

Table 5 summarizes the different models used in the explanation of crushing strength and friability of tablets. We tried to keep the models, which are here only curve fittings, as simple as possible. The linear and quadratic models proved to be good enough.

Dependence of crushing strength and friability of tablets as a functino of a few calculated compression parameters are given in Figs. 4–9. These figures are only examples. The selection of different curve fittings used in the figures may seem questionable. For example, in Fig. 4 it would have been possible to describe the crushing strength with a linear model or friability with a quadratic model. It is evident that all dependences studied here are more or less exponential, but within the experimental region used, these simple curve fittings gave as good correlation coefficients as more complicated models. All these example figures show a very high negative correlation between crushing strength and friability of tablets, which in this type of materials is quite evident.

The effects of compression time and maximum effective compression force on four calculated force–displacement parameters are given in Figs. 10 and 11. According to Fig. 10, the two responses are almost independent of compression time with low compression forces. With higher compression forces both responses are more dependent on compression times. The highest values were achieved when a slow compression speed and a high compression force were used. It is surprising that the fraction of irreversible changes increases (lower Fig. 10), especially with higher compression forces. This indicates that with low compression forces, all irreversible changes (which are possible in this material) occur rapidly. These may include rapid rearrangement and fragmentation of particles, and a certain amount of plastic deformation. With higher compression forces, melting of material at the contact points as well as plastic flow assumingly increase. These phenomena will need more time.

The two responses shown in Fig. 11 behave differently from those presented in Fig. 10, being practically independent of the compression time. This is also important, showing that these different parameters are able to provide different information on the compression phenomena.

On the basis of this study we believe that many compression parameters—like the ones presented here—can, in certain cases alone, but more presumably together, give new possibilities for understanding and also estimating the behavior of powders during compression. Later it may be possible to predict the properties of tablets even in cases where the parameterization of the compression curves is made using an eccentric tablet

Table 5

Pearson Correlation Coefficients (R) and Corresponding p Values for Crushing Strength and Friability of Tablets. (p Values Are Given Only If They Are Less Than 5%)

	Crushing Strength			Friability		
Parameter	R	p	M[a]	R	p	M[a]
$s_{FWeff,max}$	0.299	—		-0.320	—	
$Rs_{FWeff,max}$	-0.615	0.0190	L	0.595	0.0247	L
$RFD_{Q75,Feff,max}$	-0.478	—	L	0.462	—	L
$RFD_{Q50,Feff,max}$	-0.617	0.0192	L	0.602	0.0227	L
$RFD_{Q25,Feff,max}$	-0.659	0.0103	L	0.643	0.0130	L
$RFI_{Q75,Feff,max}$	0.805	0.0006	L	-0.784	0.0009	L
$RFI_{Q50,Feff,max}$	0.869	0.0001	L	-0.856	0.0001	L
$RFI_{Q25,Feff,max}$	0.898	0.0000	L	-0.884	0.0000	L
$F_{eff,max}$	0.974	0.0000	Q	-0.972	0.0000	Q
$F_{Weff,max}$	0.972	0.0000	Q	-0.946	0.0000	L
$NF_{Weff,max}$	-0.805	0.0000	Q	0.783	0.0009	L
W_{eff}	0.964	0.0000	Q	-0.923	0.0000	L
R_{FD}	0.925	0.0000	Q	-0.930	0.0000	Q
$NRFD_{Q75}$	-0.972	0.0000	Q	0.961	0.0000	Q
$NRFD_{Q50}$	-0.970	0.0000	Q	0.959	0.0000	Q
$NRFD_{Q25}$	-0.969	0.0000	Q	0.958	0.0000	Q
$NRFI_{Q75}$	-0.972	0.0000	Q	0.966	0.0000	Q
$NRFI_{Q50}$	-0.978	0.0000	Q	0.985	0.0000	Q
$NRFI_{Q25}$	-0.976	0.0000	Q	0.963	0.0000	Q
$R75_{FI,FD}$	-0.701	0.0052	L	0.689	0.0064	L
$R50_{FI,FD}$	-0.794	0.0007	L	0.782	0.0010	L
$R25_{FI,FD}$	-0.865	0.0001	L	0.852	0.0001	L
Ns_1	-0.423	—	L	0.400	—	L
Ns_2	-0.558	0.0380	Q	0.544	0.0442	Q
φ_1	-0.767	0.0014	L	0.741	0.0024	L
φ_2	0.770	0.0013	L	-0.742	0.0024	L
S_{REL}	0.693	0.0060	L	-0.669	0.0092	Q

[a]Linear model (L): f(x) = $ax + b$. Quadratic model (Q): $f(x) = ax^2 + bx + c$. a, b, c are different constants.

machine and the final compression studies with high-speed rotary machines. Also the use of compaction simulators may give more detailed information on the compression and compaction phenomena. This will inevitably require extensive work with different types of materials and proper modeling in a multidimensional space. As a matter of fact, we are actually operating with this problem, testing the use of neural networks.

CONCLUSIONS

Characterization of tablet compression force–displacement curves seems to be still too limited. Modern instrumentation and calculation techniques give new possibilities for much wider and accurate research. Today it is possible to determine a great number of parameters like the ones presented here, which describe the com-

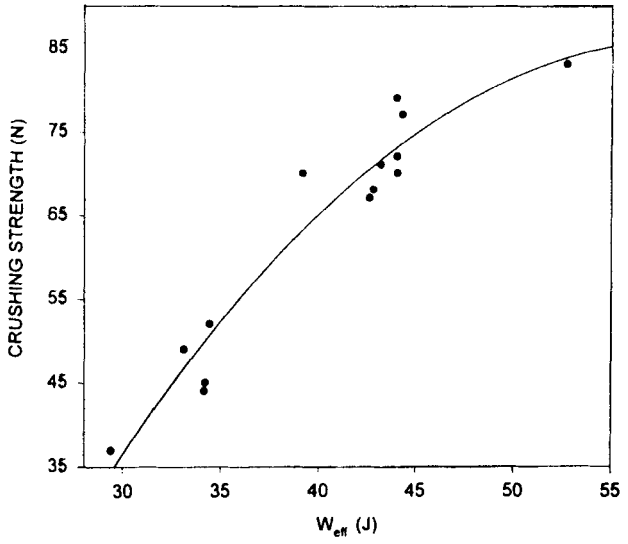

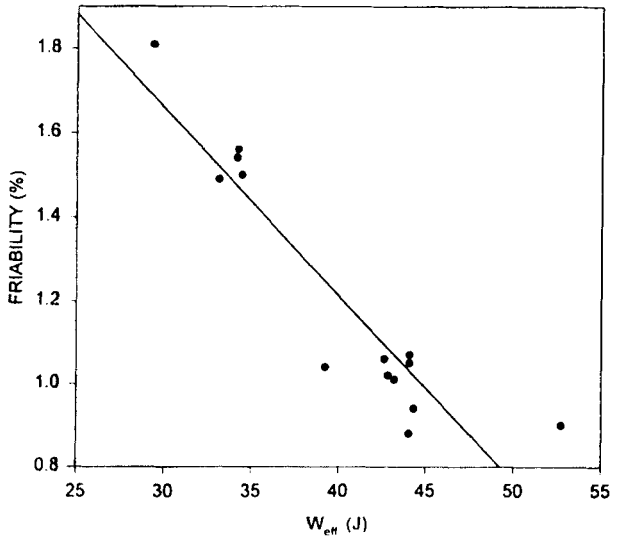

Figure 4. Dependence between effective work (W_{eff}) and the two tablet properties.

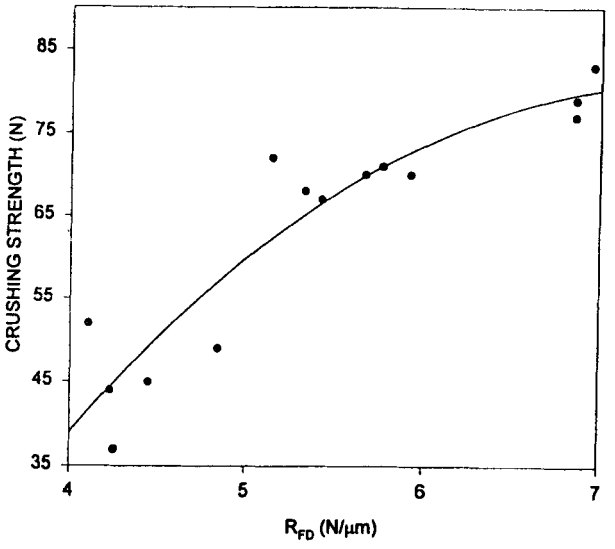

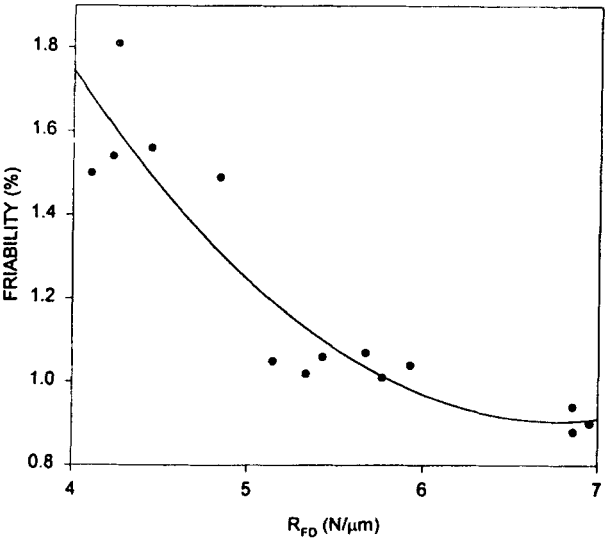

Figure 5. Dependence between force–displacement ratio (R_{FD}) and the two tablet properties.

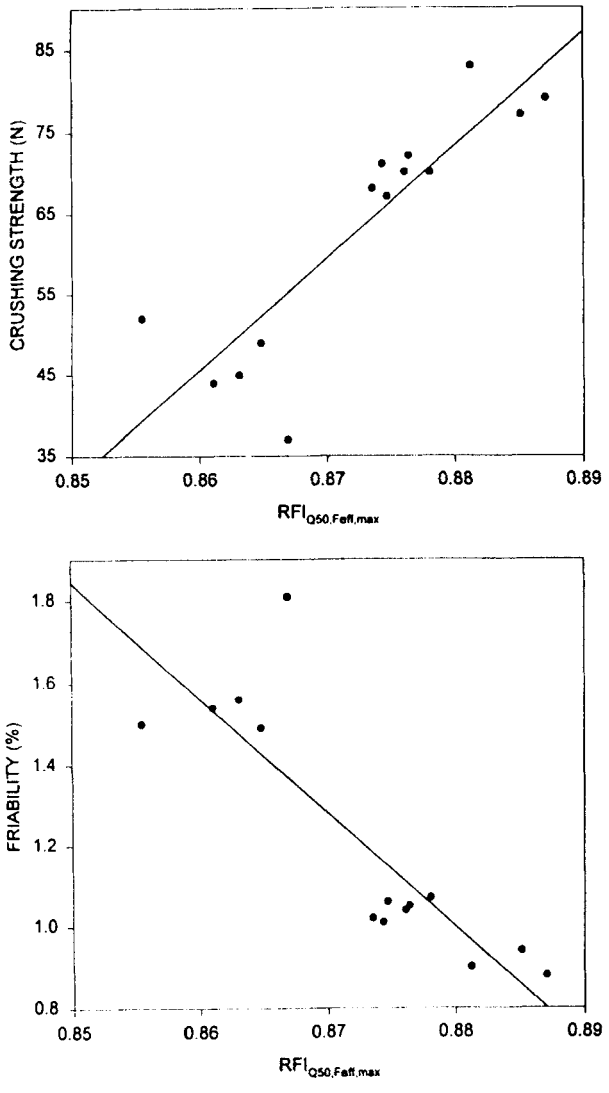

Figure 6. Dependence between 50% quartile ratio of the FI curve ($RFI_{Q50,Feff,max}$) and the two tablet properties.

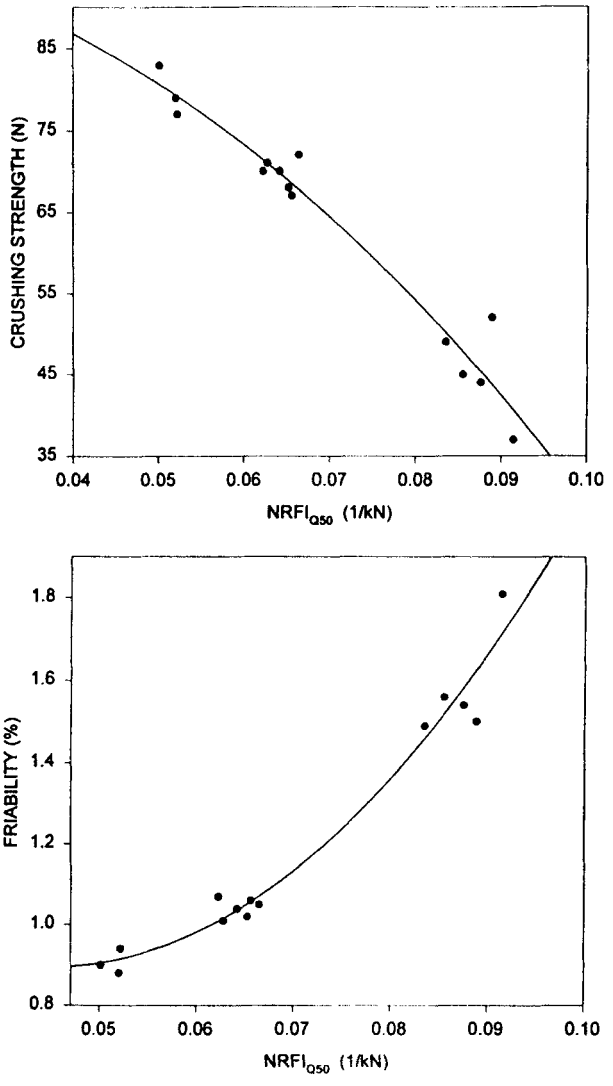

Figure 7. Dependence between 50% normalized ratio of the FI curve ($NRFI_{Q50}$ 50%) and the two tablet properties.

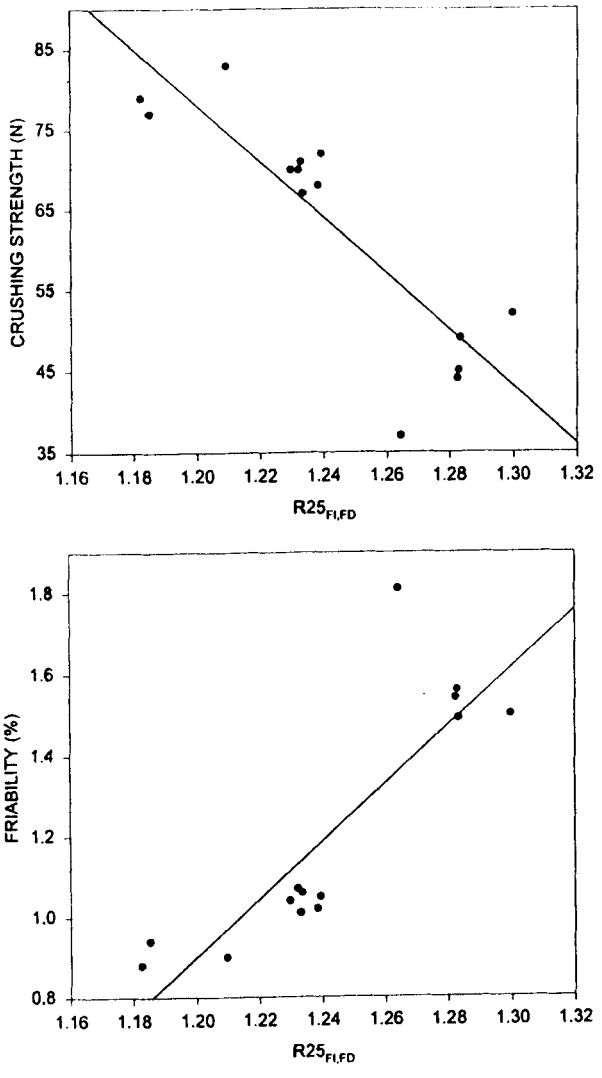

Figure 8. Dependence between the ratio of the first quartile ($R25_{FI,FD}$) and the two tablet properties.

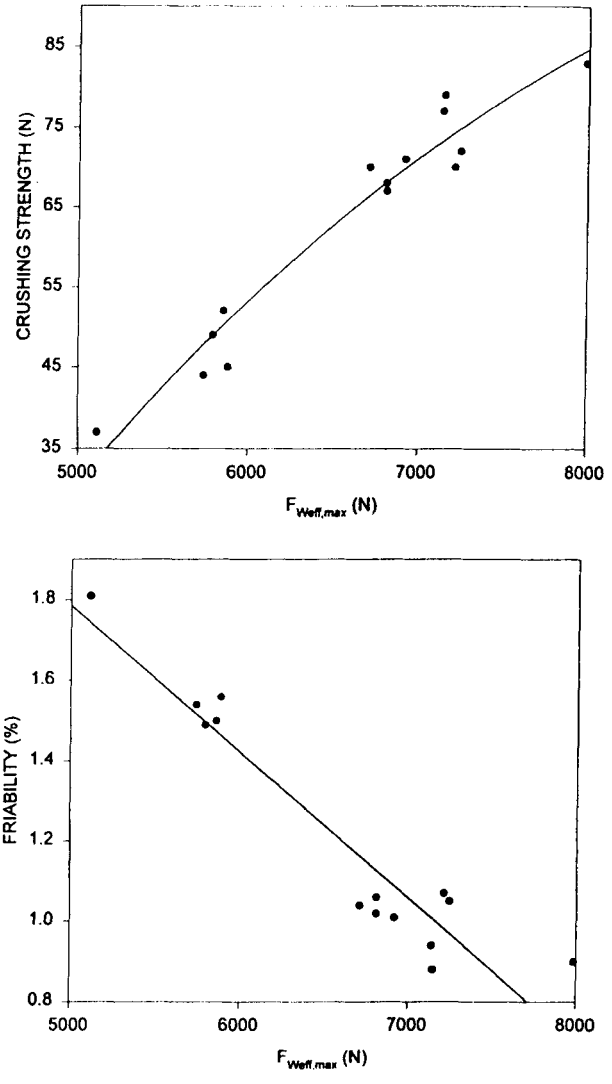

Figure 9. Dependence between the maximum force of the F_{Weff} curve ($F_{Weff,max}$) and the two tablet properties.

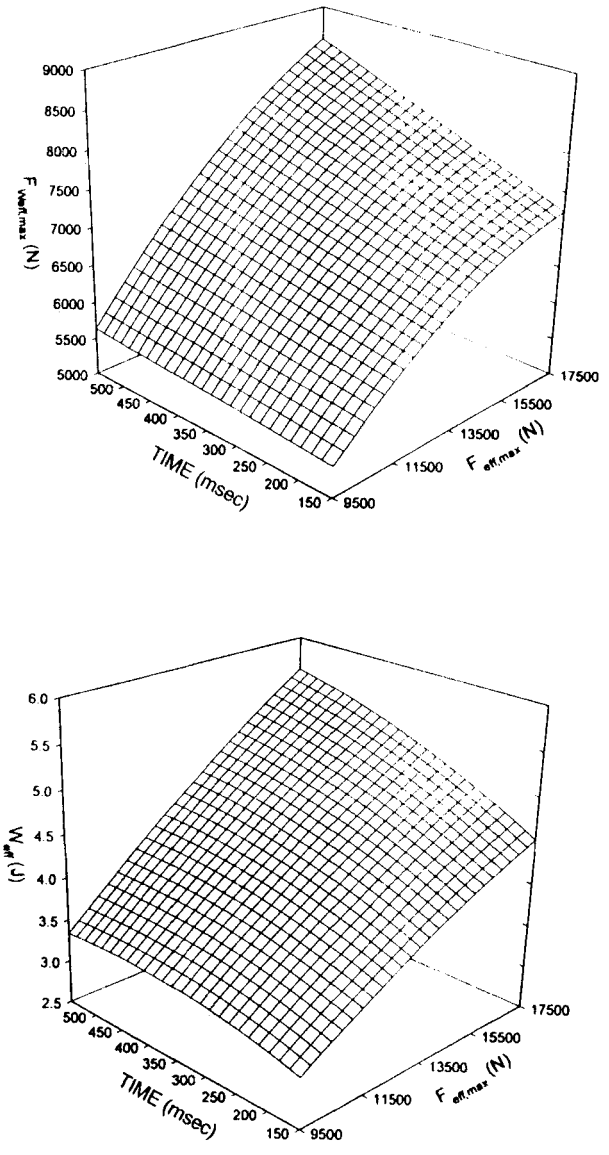

Figure 10. Effect of compression time and the maximum effective compression force on two calculated force–displacement parameters ($F_{weff,max}$ and W_{eff}).

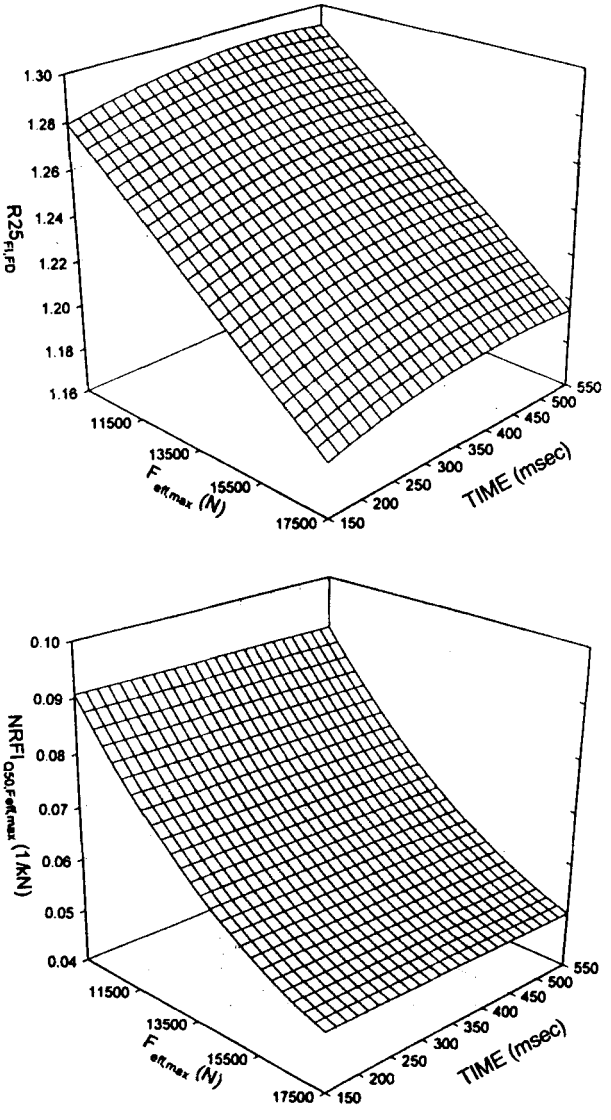

Figure 11. Effect of compression time and the maximum effective compression force on two calculated force–displacement parameters ($R25_{FI,FD}$ and $NRFI_{Q50,Feff,max}$).

pression behavior of powders from different points of view. Presumably, new data-analyzing techniques like neural networks can be used in predicting the properties of tablets on the basis of compression data.

REFERENCES

1. R. N. Chilamkurti, C. T. Rhodes, and J. B. Schwartz, Drug. Dev. Ind. Pharm., 8, 63 (1982).
2. R. N. Chilamkurti, C. T. Rhodes, and J. B. Schwartz, Pharm. Acta. Helv., 58, 146 (1983).
3. R. N. Chilamkurti, J. B. Schwartz, and C. T. Rhodes, Pharm. Acta. Helv., 58, 251 (1983).
4. R. Martinez-Pacheco, J. L. Vila-Jato, C. Souto, and J. L. Gómez-Amoza, Drug. Dev. Ind. Pharm., 16, 231 (1990).
5. U. Bogs and H. Moldenhauer, Pharmazie, 78, 704 (1963).
6. T. Tiguchi, R. D. Arnold, S. J. Tucker, and L. W. Busse, J. Am. Pharm. Assoc. Sci. Ed., 41, 93 (1952).
7. J. Hofer and F. Gstarner, Pharm. Ind., 26, 162 (1964).
8. J. Polderman, C. J. DeBlaey, D. R. Braakman, and H. Burger, Pharm. Week Bl., 104, 575 (1969).
9. J. R. Hoblitzell and C. T. Rhodes, Drug. Dev. Ind. Pharm., 16, 201 (1990).
10. H. Moldenhauer, H. Kala, G. Zessin, and M. Dittgen, Pharmazie, 35, 714 (1980).
11. G. Ragnarson and J. Sjogren, J. Pharm. Pharmacol., 37, 145 (1985).
12. K. Marshall, in *The Theory and Practice of Industrial Pharmacy* (L. Lachman, H. A. Lieberman, and J. L. Kanig, eds.), Lea & Febiger, Philadelphia, 1986, p. 66.